ANATOMIC AND COMPUTED TOMOGRAPHIC ATLAS OF THE HEAD OF THE NEWBORN BOTTLENOSE DOLPHIN (*TURSIOPS TRUNCATUS*)

Fernando Liste, Jorge Palacio, Vicente Ribes, Ana Álvarez-Clau, Luisa Fernández Domínguez, Juan Manuel Corpa

The head of a newborn dolphin (*Tursiops truncatus*), that died shortly after birth was imaged using computed tomography (CT). Gross cross-sectional slices of the head were compared with the CT images to identify normal structures of the cranium, brain, and respiratory and digestive pathways. Labelled transverse CT images of the dolphin head are presented sequentially as a reference for normal anatomy. *Veterinary Radiology & Ultrasound, Vol. 47, No. 5, 2006, pp 453–460.*

Key words: air sacs, anatomy, computed tomography, cranium, dolphin, head, nasal cavity.

Introduction

Dolphins are the subject of increasing interest with respect to diagnostic imaging techniques in the evaluation of diseases of aquatic mammals. Several articles concerning the computed tomographic (CT) and magnetic resonance (MR) imaging appearance of some normal body areas of the dolphin have been published.[1–11] An issue of special interest is the study of anatomic structures of importance to hearing and echolocation in dolphins.[3,12] To our knowledge, a complete report on the CT anatomy of the head of the dolphin has not been published. The objective of this study was to produce an atlas of CT anatomy (cross-sectional imaging) of the head of the neonatal bottlenose dolphin (*Tursiops truncatus*).

Materials and Methods

A dead newborn dolphin was donated from a local Aquarium for study purposes to the Cardenal Herrera University Veterinary Hospital. The dolphin was born normally but drowned shortly after birth. A postmortem examination of the specimen was not immediately performed due to a permit delay from the aquarium and the dolphin was kept frozen at −20°C. Two days later, the frozen specimen was subjected to a radiographic study obtaining lateral and ventrodorsal views of the head. CT imaging of the head was also performed the same day. The dolphin was placed in sternal recumbency with the head directed toward the gantry. Then, transverse 2-mm-thick CT images were acquired from the atlanto-occipital joint to the most rostral part of the nose. To compare anatomic and imaging findings, frozen transverse sections of the head were also obtained. Several slices of tissue (3 cm wide) were obtained using the same anatomical references as for CT imaging.

Results

The results of our study are shown as the matched photographs presented in the figures. Figure 1 shows a radiographic lateral view of the dolphin head acquired while

Fig. 1. Lateral radiograph of a newborn dolphin skull. Numbered lines indicate the approximate levels of each computed tomography image and anatomic slice of the frozen cadaver.

From the Dpto. Medicina y Cirugía Animal (Liste, Palacio, Álvarez-Clau) and the Dpto. Atención Sanitaria, Salud, Pública y Sanidad Animal (Corpa), Facultad de Ciencias Experimentales y de la Salud. Universidad Cardenal Herrera-CEU, Edificio Seminario, s/n. 46113 Moncada, Valencia, Spain, the Hospital Clínico Veterinario "La Marina Alta", Veterinario Parque de Animales "Mundomar", Carretera de Denia-Ondara, km 1, 03700 Denia, Valencia, Spain (Ribes), and the Emergencias Veterinarias Giorgeta, Av. Giorgeta 5. 46005 Valencia, Spain.(Domínguez)

Address correspondence and reprint requests to Fernando Liste, at the above address.

E-mail: fernandoxy@yahoo.com

Received July 22, 2005; accepted for publication January 25, 2006.

doi: 10.1111/j.1740-8261.2006.00167.x

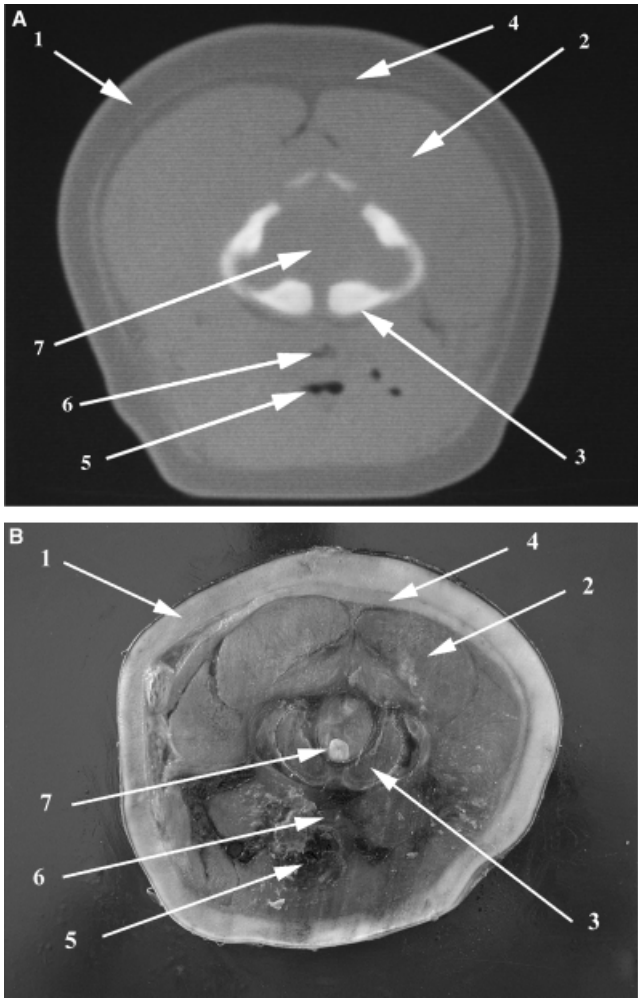

FIG. 2. Computed tomography image (A) and caudal surface of anatomic section (B) made at level 2: (1) blubber; (2) Ms. semispinalis capitis; (3) occipital condyles; (4) subdermal adipose tissue; (5) trachea; (6) esophagus; (7) medulla oblongata.

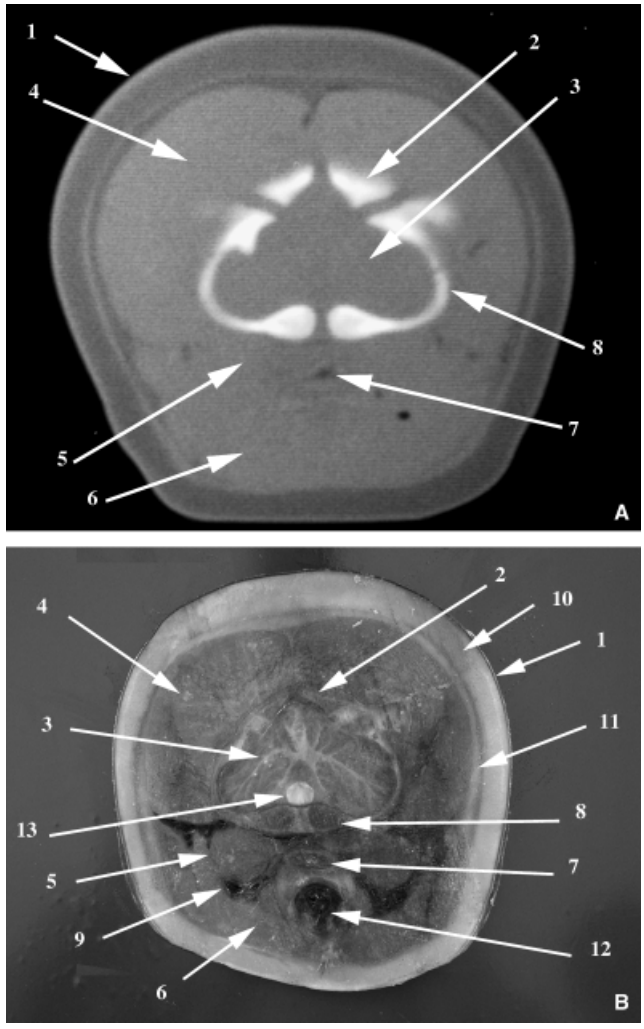

FIG. 3. Computed tomography image (A) and caudal surface of anatomic section (B) made at level 3: (1) epidermis; (2) external occipital protuberance; (3) cerebellum; (4) Ms. semispinalis capitis; (5) Ms. scalenus; (6) Ms. sternohyoideus; (7) esophagus; (8) occipital bone; (9) external jugular vein; (10) blubber; (11) subdermal adipose tissue; (12) trachea; (13) medulla oblongata.

the specimen was placed in lateral recumbency. The lines in Fig. 1 represent the approximate levels of each CT image and anatomic slice of the cadaver. In Figs. 2–14, the CT image (A) and the cut surface of the anatomic slice (B) are viewed sequentially from caudal to rostral. All transverse CT images and anatomic slices are oriented with the left aspect of the head to the reader's right. Bone window CT images were used in this anatomic atlas.

Discussion

CT is an excellent modality to explore dense structures such as the temporal bones (Fig. 6A). CT is superior compared with conventional radiography because overlying structures impede examination of the skull. All skull and hyoid bones were easily identified on CT images. However, the hyoid apparatus is seen at a different level on the gross slices (compare Fig. 6A with Figs. 9B, and Fig. 10B, respectively). We believe this is due to a slightly different cut angle for gross slices of the frozen cadaver compared with the CT images. Sutures from flat bones in the cranium were occasionally detected in this newborn specimen (Figs. 3A, 4A and 7A, 9A). The melon, a bulbous fatty substance located immediately rostral to the forebrain (Figs. 12A and 13A), serves as an acoustic lens and focuses vocalized clicks into a narrow beam. Other structures important to hearing and echolocation such as the middle ear complex and some air sacs were also located (Figs. 12A and 13A).

The CT procedure was performed 2 days after death on a frozen specimen. Thus, postmortem changes can be appreciated in some CT images appearing as a small amount

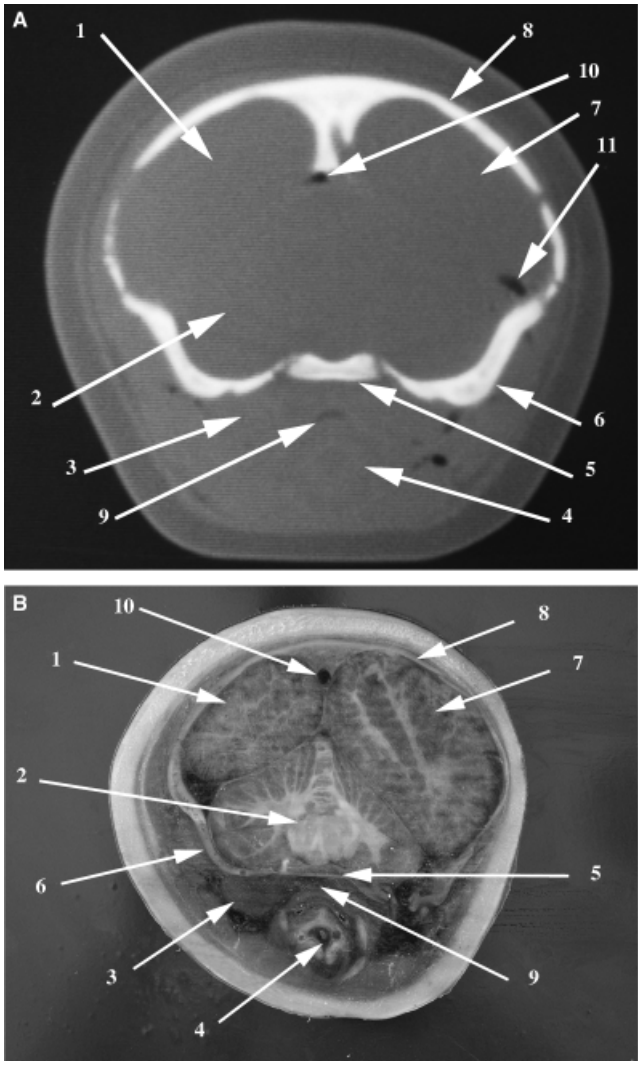

FIG. 4. Computed tomography image (A) and caudal surface of anatomic section (B) made at level 4: (1) occipital lobe; (2) cerebellum; (3) Ms. scalenus; (4) larynx; (5) basioccipital; (6) Os temporale; (7) parietal lobe; (8) Os parietale; (9) esophagus; (10) sinus sagittalis dorsalis; (11) gas artifact.

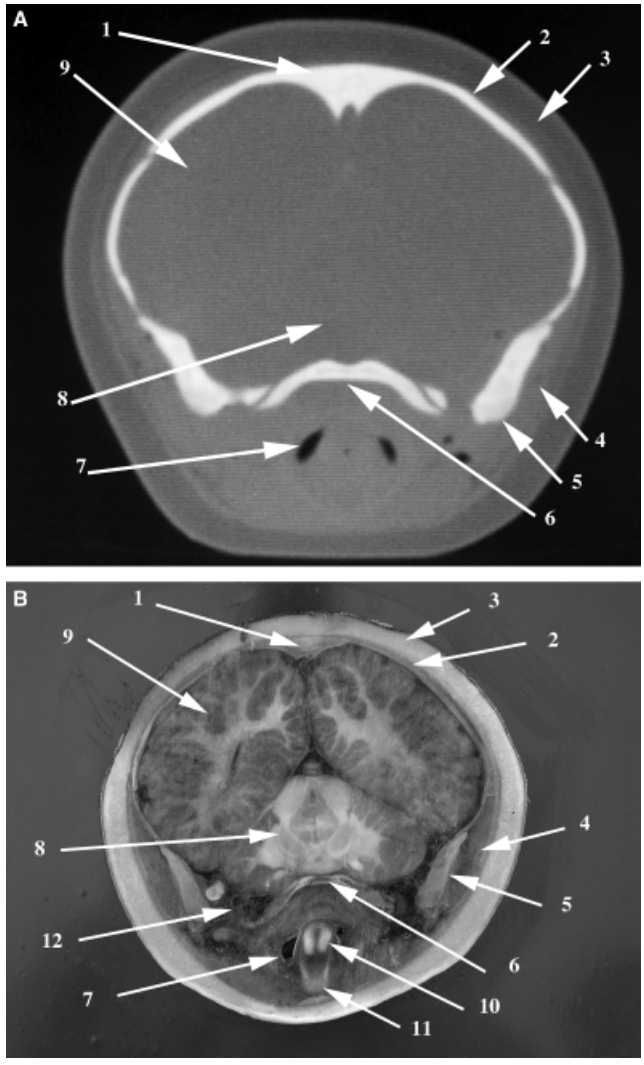

FIG. 5. Computed tomography image (A) and caudal surface of anatomic section (B) made at level 5: (1) pars supraoccipitalis; (2) Os parietalis; (3) blubber; (4) Ms. temporalis; (5) Os temporalis; (6) pars basioccipitalis; (7) esophagus; (8) cerebellum; (9) parietal lobe; (10) processus cuneiformis; (11) epiglottic cartilage; (12) internal carotide artery.

of gas in some brain areas (Fig. 4A) and inside small arteries such as the internal carotid arteries (Figs. 8A and 9A).

This anatomic guide can be used as a reference in understanding the anatomic features of the dolphin head.

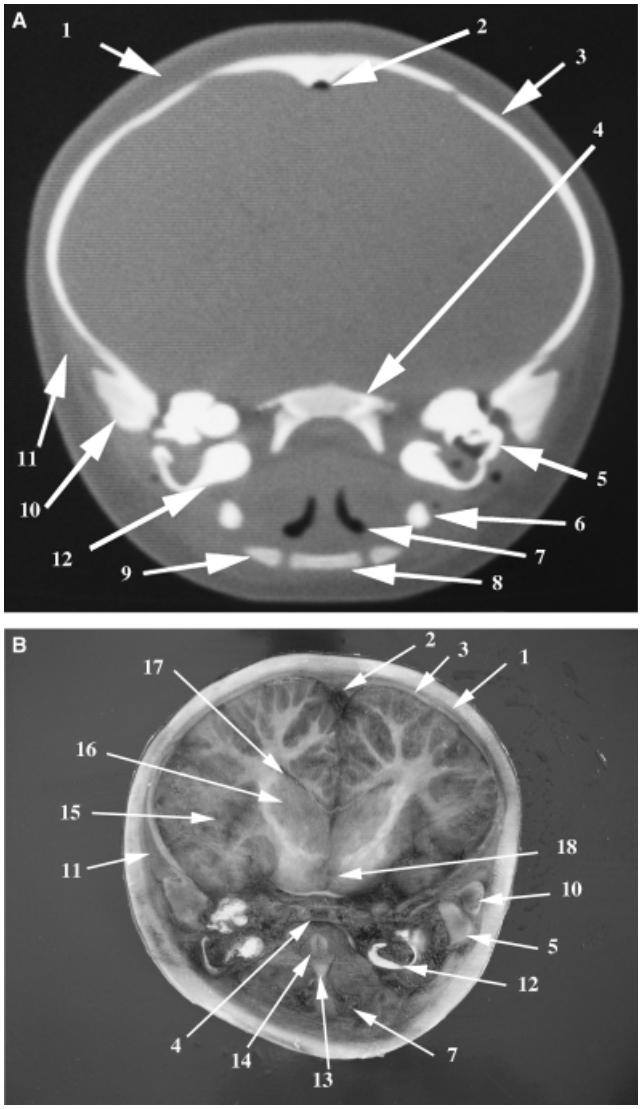

FIG. 6. Computed tomography image (A) and caudal surface of anatomic section (B) made at level 6: (1) blubber; (2) sinus sagitalis dorsalis; (3) Os parietale; (4) Os basisphenoideum; (5) Os temporalis, squamous part; (6) Os ceratohyoideum; (7) oral part of the pharynx; 8) Os basihyoideum; (9) Os stylohyoid; (10) Os temporalis, zygomatic process; (11) Ms. temporalis; (12) Os temporalis, tympanic part; (13) epiglottic cartilage; (14) processus cuneiformis; (15) corpus striatum; (16) thalamus; (17) lateral ventriculum; (18) pituitary gland.

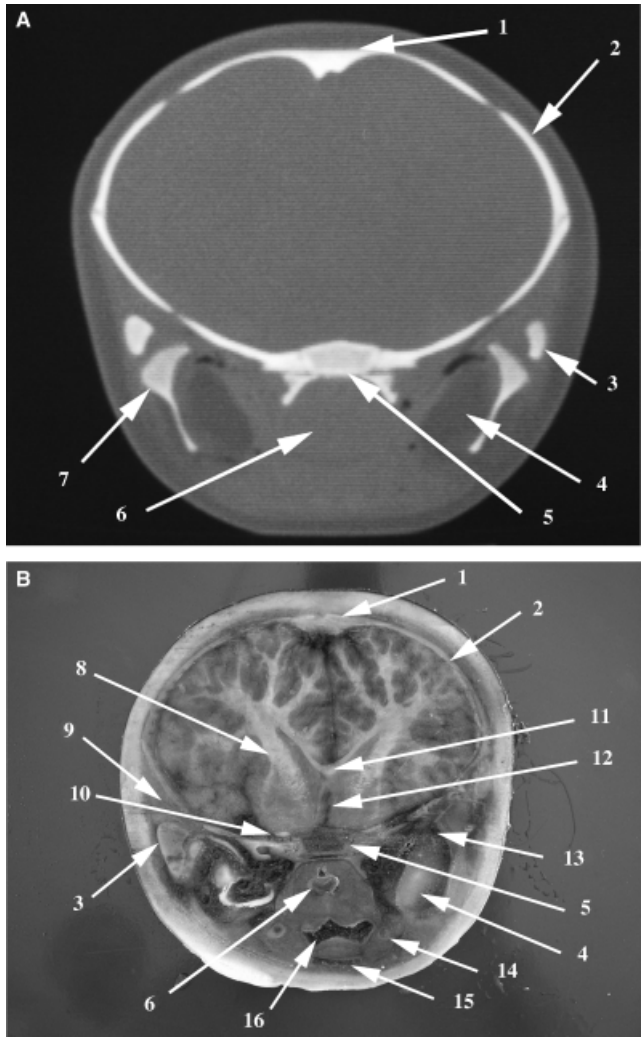

FIG. 7. Computed tomography image (A) and caudal surface of anatomic section (B) made at level 7: (1) Os occipitale: pars supraoccipitalis; (2) Os parietale; (3) Os temporalis, zygomatic process; (4) mandibula bulba; (5) Os basisphenoid; (6) pharynx: pars nasalis; (7) corpus mandibulae; (8) corpus striatum; (9) Ms. maseter; (10) optical nerve; (11) corpus callosum; (12) septum pellucidum; (13) internal carotid artery; (14) Os ceratohyoideum; (15) Os basihyoideum; (16) pharynx, pars oralis.

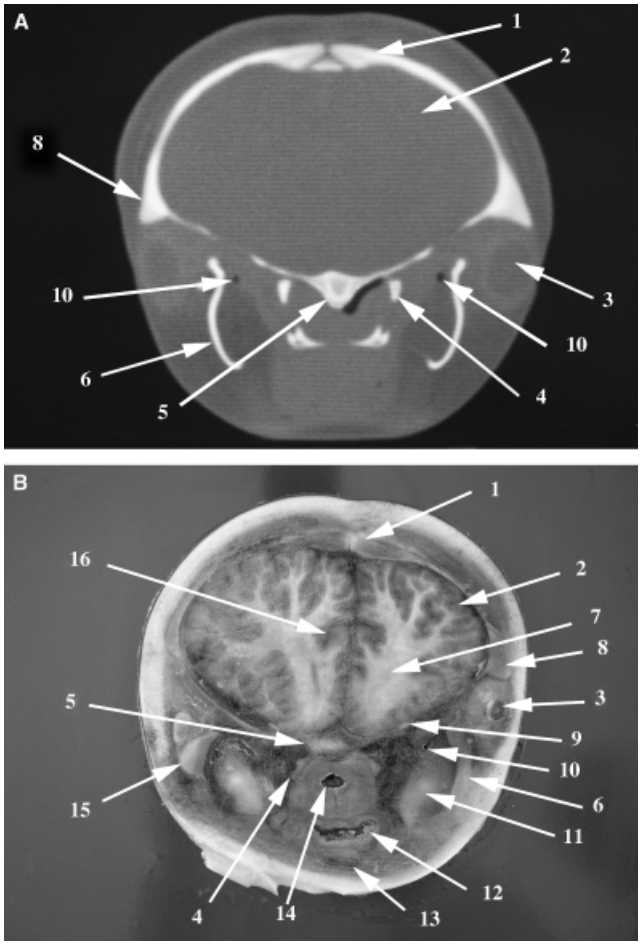

FIG. 8. Computed tomography image (A) and caudal surface of anatomic section (B) made at level 8: (1) Os Occipitale: pars supraoccipitalis; (2) cortex cerebri; (3) eyeball; (4) Os pterygoideum; (5) Os vómer; (6) corpus mandibulae; (7) internal capsule; (8) Os zygomaticum; (9) optical nerve; (10) internal carotid artery; (11) mandibula bulba; (12) pharynx, pars oralis; (13) Os basihyoideum; (14) pharynx: pars nasalis; (15) Os temporalis, zygomatic process; (16) lateral ventriculus.

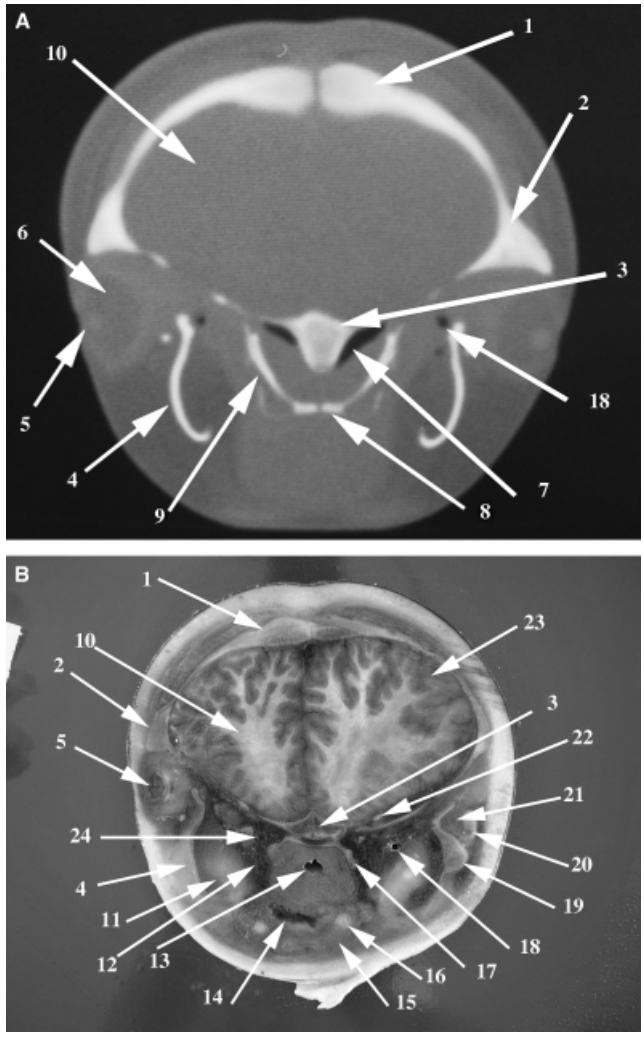

FIG. 9. Computed tomography image (A) and caudal surface of anatomic section (B) made at level 9: (1) Os occipitale: pars supraoccipitalis; (2) Os zygomaticus; (3) Os vomer; (4) corpus mandibulae; (5) lens; 6) vitreus; (7) nasal meatus; (8) Os palatinum; (9) Os maxilla: palatinum process; (10) cerebrum: frontal lobe; (11) mandibula bulba; (12) Ms. pterygoideus; (13) pharynx: pars nasalis; (14) pharynx, pars oralis; (15) Ms. genihyoideus; (16) Os stylohyoideum; (17) Os pterygoideum; (18) internal carotid artery; (19) Os temporale: pars squamosa; (20) Os temporale; zygomaticus process; (21) Ms. maseterus; (22) optical nerve; (23) cortex cerebri; (24) sinus venosus ethmoidalis.

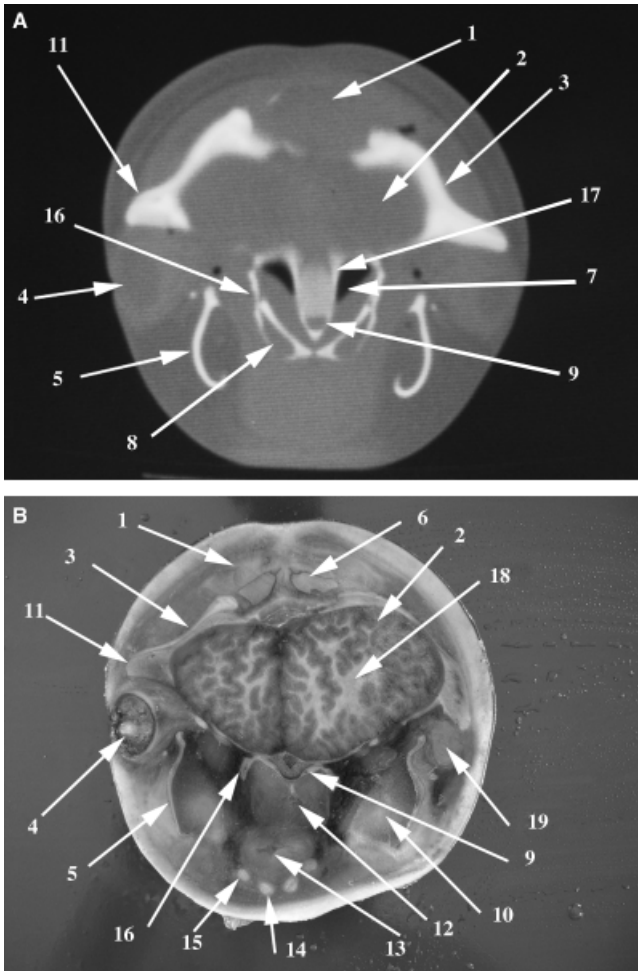

FIG. 10. Computed tomography image (A) and caudal surface of anatomic section (B) made at level 10: (1) nasal plug muscle; (2) frontal lobe; (3) Os maxilla; (4) eyeball; (5) corpus mandibulae; (6) nasal plug; (7) meatus nasalis; (8) sinus venosus maxillaris; (9) Os vomer; (10) mandibula bulba; (11) Os zygomaticum; (12) pharynx: pars nasalis; (13) pharynx, pars oralis; (14) Os ceratohyoideum; (15) Os stylohiodeum; (16) Os pterygoideum; (17) Os nasale; (18) capsula interna; (19) ocular muscles.

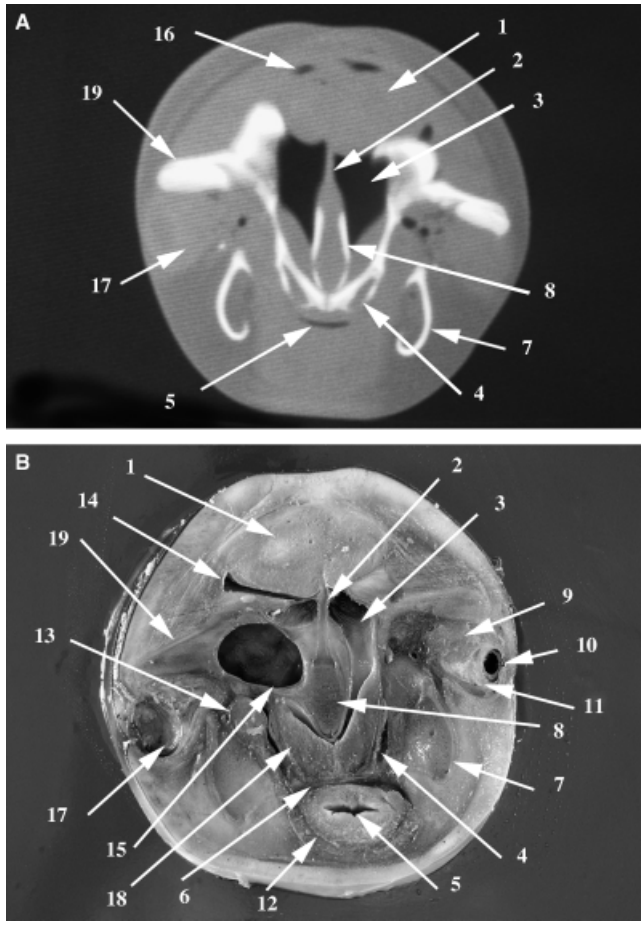

FIG. 11. Computed tomography image (A) and caudal surface of anatomic section (B) made at level 11: (1) melon fatty bursae; (2) septum nasi; (3) meatus nasalis; (4) sinus maxillaris; (5) pharynx, pars oralis; (6) Os palatinum; (7) corpus mandibulae; (8) Os nasum; (9) Ms. rectum dorsi; (10) lens; (11) sclera; (12) Ms. genioglossus; (13) Ms. pterygoideus; (14) saccus nasofrontalis dorsalis; (15) saccus nasofrontalis ventralis; (16) saccus vestibularis; (17) vitreus; (18) concha nasalis ventralis; (19) Os maxilla.

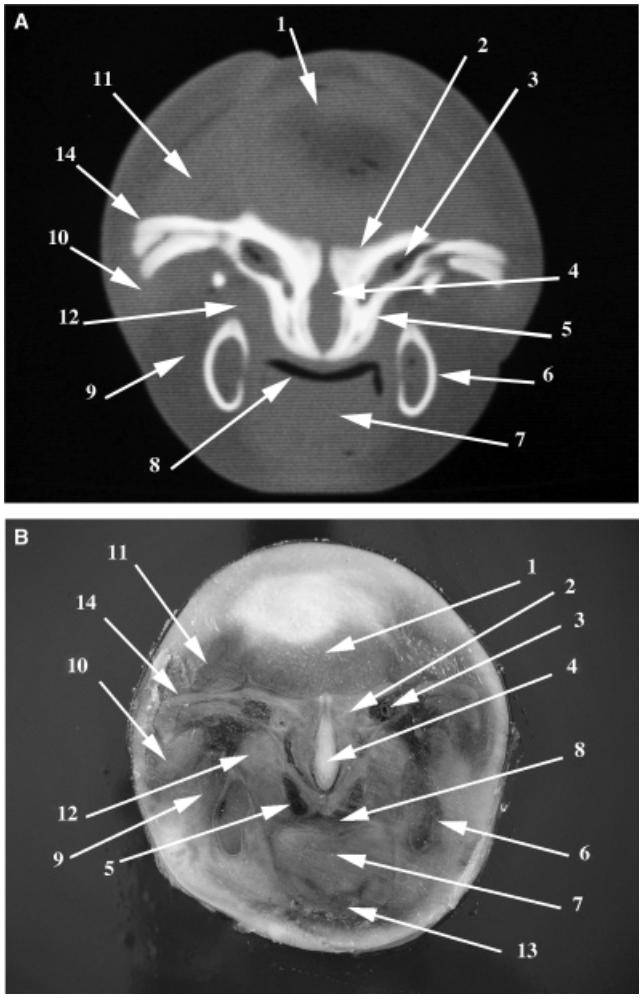

FIG. 12. Computed tomography image (A) and caudal surface of anatomic section (B) made at level 12: (1) melon fatty bursae; (2) Os nasum; (3) sinus ethmoidalis; (4) internasal cartilage; (5) sinus maxillaries; (6) corpus mandibulae; (7) tongue; (8) oral cavity; (9) Ms. maseterus; (10) Ms. cutaneum labiorum; (11) Ms. rostralis lateralis; (12) Ms. pterigoideus; (13) Ms. milohyoideus; (14) Os maxilla.

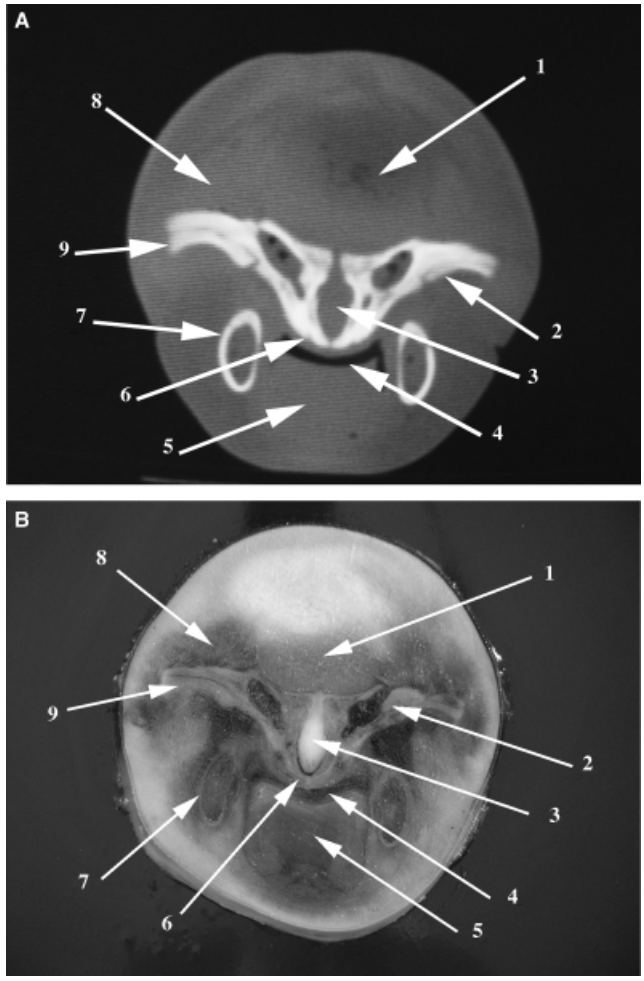

FIG. 13. Computed tomography image (A) and caudal surface of anatomic section (B) made at level 13: (1) melon fatty bursae; (2) Os maxilla; (3) internasal cartilage; (4) oral cavity; (5) tongue; (6) Os vomer; (7) corpus mandibulae; (8) Ms. rostralis lateralis; (9) Os zygomaticum.

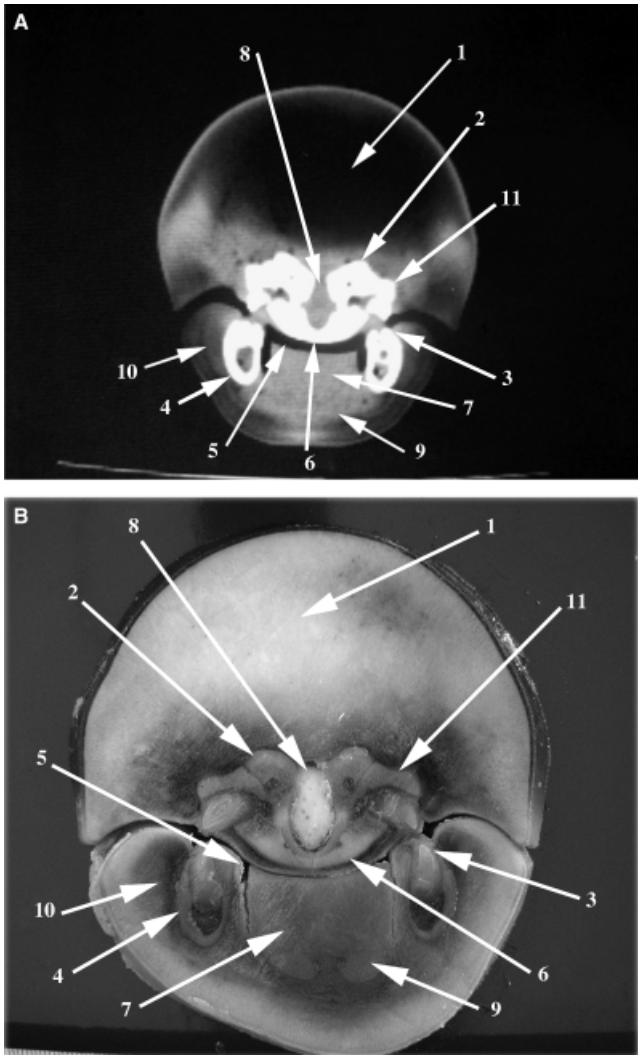

FIG. 14. Computed tomography image (A) and caudal surface of anatomic section (B) made at level 14: (1) blubber; (2) Os nasum; (3) right lower teeth; (4) mandibulae; (5) oral cavity; (6) Os maxilla: palatine process; (7) tongue; (8) cartilage intermaxillaris; (9) basilingual muscles; (10) Ms. cutaneous labiorum; (11) Os maxilla.

REFERENCES

1. Marino L, Murphy TL, Deweerd AL, et al. Anatomy and three-dimensional reconstructions of the brain of the white whale (*Delphinapterus leucas*) from magnetic resonance images. Anat Rec 2001;262:429–439.

2. Zucca P, Di Guardo G, Pozzi-Mucelli R, Scaravelli D, Francese M. Use of computer tomography for imaging of *Crassicauda grampicola* in a Risso's dolphin (*Grampus griseus*). J Zoo Wild Med 2004;35:391–394.

3. Houser DS, Finneran J, Carder D, et al. Structural and functional imaging of bottlenose dolphin (*Tursiops truncatus*) cranial anatomy. J Exp Biol 2004;207(Part 21):3657–3665.

4. Finneran JJ. Whole-lung resonance in a bottlenose dolphin (*Tursiops truncatus*) and white whale (*Delphinapterus leucas*). J Acoust Soc Am 2003;114:529–535.

5. Marino L, Sudheimer K, McLellan WA, Johnson JI. Neuroanatomical structure of the spinner dolphin (*Stenella longirostris orientalis*) brain from magnetic resonance images. Anat Rec A Discov Mol Cell Evol Biol July 2004;279:601–610.

6. Marino L, Sudheimer K, Pabst DA, McLellan WA, Johnson JI. Magnetic resonance images of the brain of a dwarf sperm whale (*Kogia simus*). J Anat 2003;203:57–76.

7. Marino L, Sudheimer K, Sarko D, Sirpenski G, Johnson JI. Neuroanatomy of the harbor porpoise (*Phocoena phocoena*) from magnetic resonance images. J Morphol 2003;257:308–347.

8. Marino L, Sudheimer KD, Pabst DA, McLellan WA, Filsoof D, Johnson JI. Neuroanatomy of the common dolphin (*Delphinus delphis*) as revealed by magnetic resonance imaging (MRI). Anat Rec 2002;268:411–429.

9. Marino L, Murphy TL, Gozal L, Johnson JI. Magnetic resonance imaging and three-dimensional reconstructions of the brain of a fetal common dolphin, *Delphinus delphis*. Anat Embryol (Berlin) 2001; 203:393–402.

10. Fraser FC, Purves PE. Anatomy and function of the cetacean ear. Proc R Soc Lond B Biol Sci 1960;152:62–77.

11. Corpa JM, Peris B, Palacio J, Liste F, Ribes V. Hydrocephalus in a newborn bottlenosed dolphin (*Tursiops truncatus*). Vet Rec 2004;155:208–210.

12. Cranford TW, Amundin M, Norris KS. Functional morphology and homology in the odontocete nasal complex: implications for sound generation. Morphol 1996 Jun;228:223–285.